Tests of the quantum superposition principle: current experiments on Earth, future experiments in Space

Matteo Carlesso and Angelo Bassi*

Department of Physics, University of Trieste,
Strada Costiera 11, 34151 Trieste, Italy
**E-mail: abassi@units.it*
www.units.it

The superposition principle is the building block of quantum mechanics, the theory we use to describe the behavior of light and matter - at least in the microscopic domain. It means that systems can be in two or more different states at once, and this precisely makes quantum theory so radically different from classical mechanics. Why quantum properties of atoms and molecules seem not to carry over to macroscopic systems is a major open question, and model have been developed, which implement a progressive loos of quantum coherence when the mass and complexity of the system increase. We will review such models, as well as current attempts to test the loss of quantum coherence they predict. Such experiments range from matter-wave interferometry, to cold atoms, to optomechanical setups, and more. The next frontier will be space, where the quantum properties of systems, which are way larger than what is possible on Earth, can be tested.

Keywords: Quantum Coherence, Collapse Models, Optomechanics, Space Missions

1. Collapse Models for the Quantum-to-Classical Transition

Collapse models are phenomenological models aimin at describing the transition from the micro-world, well described by quantum mechanics, to the macro-world, where systems are never observed in superpositions. To this end, one adds stochastic and non-linear terms to the Schrödinger equation in such a way that the wave function collapse is embedded in the dynamics [1]. This solves the quantum measurements problem, because now the collapse becomes a universal feature of the dynamics, not something that occurs mysteriously only in measurement processes.

Collapse models have a built-in amplification mechanism which ensures that the collapse effects are small for microscopic systems in order to agree with known and experimentally verified results about quantum mechanics; at the same time they act strongly on macroscopic systems, where superpositions are suppressed and systems behave classically [2]. This coherently explains the quantum-to-classical transition, which has puzzled the scientific community since the birth of Quantum Mechanics, avoiding paradoxes like the famous Schrödinger's cat.

The best known and studied among collapse models is the Continuous Spontaneous Localization (CSL) model, which is constructed in a way that the localization occurs continuously in time. The CSL equation reads [2]:

$$\frac{\mathrm{d}|\psi_t\rangle}{\mathrm{d}t} = \left[-\frac{i}{\hbar}\hat{H} + \frac{\sqrt{\lambda}}{m_0}\int \mathrm{d}\mathbf{x}\,\left(\hat{M}(\mathbf{x}) - \langle\hat{M}(\mathbf{x})\rangle_t\right) w(\mathbf{x},t) \right.$$
$$\left. -\frac{\lambda}{2m_0^2}\int \mathrm{d}\mathbf{x}\,\left(\hat{M}(\mathbf{x}) - \langle\hat{M}(\mathbf{x})\rangle_t\right)^2\right]|\psi_t\rangle\,,$$

where m_0 is a reference mass taken equal to that of a nucleon, λ is the coupling rate between the system and the noise field allegedly responsible for the collapse, r_C is the typical correlation length for the latter, $|\psi_t\rangle$ is the N particle wavefunction, $\hat{H}$ is the system Hamiltonian, and $w(\mathbf{x},t)$ is the noise providing the collapse, characterized by $\langle w(\mathbf{z},t)\rangle = 0$ and $\langle w(\mathbf{z},t)w(\mathbf{x},s)\rangle = \delta^{(3)}(\mathbf{z}-\mathbf{x})\delta(t-s)$. The locally averaged mass density operator is defined as $\hat{M}(\mathbf{x}) = \sum_j m_j \sum_s \int \mathrm{d}\mathbf{y}\, g(\mathbf{x}-\mathbf{y})\hat{a}_j^\dagger(\mathbf{y},s)\hat{a}_j(\mathbf{y},s)$, where $\hat{a}_j^\dagger(\mathbf{y},s)$ and $\hat{a}_j(\mathbf{y},s)$ are respectively the creation and annihilation operators of a particle of type j with mass m_j and spin s, while $g(\mathbf{x}-\mathbf{y}) = (\pi^{3/4}r_C^{3/2})^{-1}\exp\left[(\mathbf{x}-\mathbf{y})^2/(2r_C^2)\right]$ is a smearing function imposing a spatial correlation on the collapses. We note that the collapse effect in Eq. (1) is mass proportional, implying that in calculations one can safely neglect the contributions from electrons and focus only on nucleons. Given the above equation, one can compute the predictions of the CSL model, whose comparison with the experimental results constrains the CSL parameter space, as we will now discuss.

2. Experimental Constrains on the CSL Parameter Space

The model is characterized by the two free parameters λ and r_C. Ghirardi, Rimini and Weber (GRW) originally set[3] $\lambda = 10^{-16}\,\mathrm{s}^{-1}$ and $r_C = 10^{-7}\,\mathrm{m}$. Later, Adler suggested different values[4] namely $r_C = 10^{-7}\,\mathrm{m}$ with $\lambda = 10^{-8\pm2}\,\mathrm{s}^{-1}$ and $r_C = 10^{-6}\,\mathrm{m}$ with $\lambda = 10^{-6\pm2}\,\mathrm{s}^{-1}$. This shows that there is no consensus so far on the actual values of the parameters. As the CSL model is phenomenological, the values of λ and r_C must be eventually determined by experiments. Although only recently the scientific community has started developing dedicated experiments[5,6], one can infer bounds on the CSL parameters by comparing the predictions of the model with available experimental data in the literature. In this respect, experiments can be grouped in two classes: interferometric tests and non-interferometric tests.

2.1. *Interferometric tests*

Interferometric tests include those experiments, which directly create and detect quantum superpositions of the center of mass of massive systems. These are the most natural test of collapse models, whose first effect is to destroy superpositions and localize the state of the system in space. By detecting the interference pattern, one can place bounds on the collapse parameters. Examples of these experiments are atom[7] and molecular[8,9] interferometry and entanglement experiment with diamonds[10]. Following the same idea, one can set also a lower bound starting from theoretical considerations[9]. Indeed, one of the request for collapse models is that macroscopic system cannot be found in a superposition, and this defines a minimum value for the coupling constant λ at given r_C. The left panel of Figure 1 shows the upper bounds obtained from interferometric experiments, compared with the GRW's and Adler's theoretically proposed values of the parameters and the lower bound.

2.2. *Non-interferometric tests*

Actually, the strongest bounds on the CSL parameters come from non-interferometric experiments, where no superposition is generated. They are sensitive to small position displacements and aim at detecting CSL-induced diffusion in position [11] and angles [12]. These experiments involve cold atoms [13], optomechanical systems [5,12,14,15], X-ray measurements [16] and phonon excitations in crystals [17]. Note that in non-interferometric experiments one can also consider systems which are (truly) macroscopic. In such a case, due to the amplification mechanism, the collapse can be more significant and easier to detect. The middle panel of Figure 1 shows the upper bounds that can be inferred from the existing non-interferometric tests.

3. The case for space

Albeit several experimental data can be used to test collapse models, the CSL parameter space still exhibits a vast unexplored region. Recently, also due to the advances in technology, various theoretical and experimental proposals were putted forward [12,18]. Among them, the space-mission MAQRO [19] has attracted strong attention from the scientific community, since if performed, the experiment should be able to cover almost fully the unexplored CSL region, well beyond the originally values proposed by GRW [3]. The idea is to perform interferometric and/or non-interferometric tests, similar to those already performed on Earth, but now in a micro-gravitational environment provided by outer space. Micro-gravity allows to increase the measurement times, thus providing a larger build-up of potential

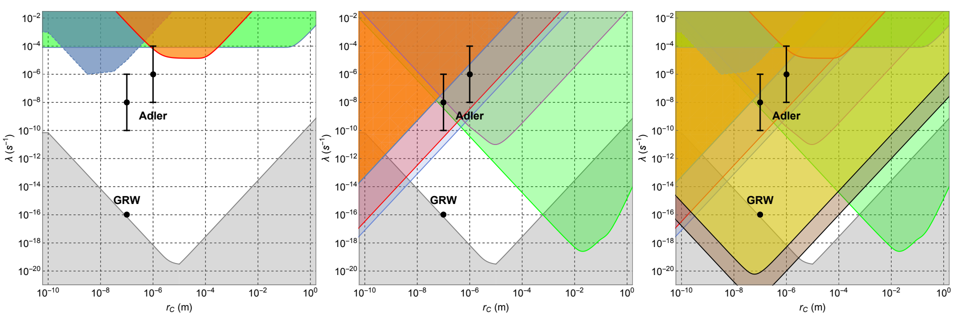

Fig. 1. Exclusion plots for the CSL parameters with respect to the GRW's and Adler's theoretically proposed values [3,4]. *Left panel* - Excluded regions from interferometric experiments: molecular interferometry [8,9] (blue area), atom interferometry [7] (green area) and experiment with entangled diamonds [10] (orange area). *Middle panel* - Excluded regions from non-interferometric experiments: LISA Pathfinder [12,14] (green area), cold atoms [13] (orange area), phonon excitations in crystals [17] (red area), X-ray measurements [16] (blue area) and nanomechanical cantilever [5]. *Right panel* - Hypothetical upper bounds from the space-mission MAQRO compared to the previous established experimental bounds: non-interferometric (yellow area) and interferometric (brown area) experiments [Credits: Rainer Kaltenbaek (Uninersity of Vienna)]. We report with the grey area the region excluded based on theoretical arguments [9].

collapse effects, which are supposed to grow with time. Also, larger masses can be employed, which further increases the collapse effect. The right panel of Figure 1 shows the wide improvement that can be achieved with MAQRO in comparison with the present experimental upper bounds on the collapse parameters.

Acknowledgments

The authors acknowledge support from the University of Trieste (FRA 2016), INFN, the COST Action QTSpace (CA15220) and the H2020 FET project TEQ (grant n. 766900).

References

1. N. Gisin, *Hel. Phys. Acta* **62**, 363 (1989); A. Bassi *et al.*, *Phys. Rev. Lett.* **111**, p. 210401 (2013).
2. G. C. Ghirardi *et al.*, *Found. Phys.* **25**, 5 (1995); A. Bassi *et al.*, *Phys. Rep.* **379**, 257 (2003); A. Bassi *et al.*, *Rev. Mod. Phys.* **85**, 471 (2013).
3. G. C. Ghirardi *et al.*, *Phys. Rev. D* **34**, 470 (1986).
4. S. L. Adler, *J. Phys. A* **40**, p. 13501 (2007); *Ibid.* **40**, p. 2935 (2007).
5. A. Vinante *et al.*, *Phys. Rev. Lett.* **116**, p. 090402 (2016); *Ibid.* **119**, p. 110401 (2017)
6. A. Bassi *et al.*, *Nuclear Physics News* **28**, p. 37 (2018).
7. T. Kovachy *et al.*, *Nature* **528**, 530 (2015).
8. S. Eibenberger *et al.*, *Phys. Chem. Chem. Phys.* **15**, 14696 (2013); K. Hornberger *et al.*, *Phys. Rev. A* **70**, p. 053608 (2004).
9. M. Toroš *et al.*, *Phys. Lett. A* **381**, 3921 (2017); *J. Phys. A* **51**, p. 115302 (2018).
10. K. C. Lee *et al.*, *Science* **334**, 1253 (2011); S. Belli *et al.*, *Phys. Rev. A* **94**, p. 012108 (2016).
11. M. Bahrami *et al.*, *Phys. Rev. Lett.* **112**, p. 210404 (2014); S. Nimmrichter *et al.*, *Ibid.* **113**, p. 020405 (2014); L. Diósi, *Ibid.* **114**, p. 050403 (2015).
12. B. Schrinski *et al.*, *J. Opt. Soc. Am. B* **34**, C1 (2017) M. Armano *et al.*, *Phys. Rev. Lett.* **120**, p. 061101 (2018); M. Carlesso *et al.*, *ArXiv*, 1708.04812 (2017).
13. T. Kovachy *et al.*, *Phys. Rev. Lett.* **114**, p. 143004 (2015); M. Bilardello *et al.*, *Phys. A* **462**, 764 (2016).
14. M. Armano *et al.*, *Phys. Rev. Lett.* **116**, p. 231101 (2016); M. Carlesso *et al.*, *Phys. Rev. D* **94**, p. 124036 (2016); B. Helou *et al.*, *Ibid.* **95**, p. 084054 (2017).
15. A. Vinante *et al.*, *Class. Quantum Grav.* **23**, p. S103 (2006); B. P. Abbott *et al.*, *Phys. Rev. Lett.* **116**, p. 061102 (2016); *Ibid.* **116**, p. 131103 (2016).
16. C. E. Aalseth *et al.*, *Phys. Rev. C* **59**, 2108 (1999); K. Piscicchia *et al.*, *Entropy* **19** (2017).
17. S. L. Adler *et al.*, *Phys. Rev. A* **97**, p. 052119 (2018); M. Bahrami, *Ibid.* **97**, p. 052118 (2018).

18. D. Goldwater *et al.*, *Phys. Rev. A* **94**, p. 010104(R) (2016); S. McMillen *et al.*, *Ibid.* **95**, p. 012132 (2017); M. Carlesso *et al.*, *ArXiv*, 1805.11037 (2018).
19. R. Kaltenbaek *et al.*, *EPJ Quantum Technology* **3**, p. 5 (2016).